

Intracellular Temperature Imaging in Gold Nanorod-Assisted Photothermal Therapy with Luminescent Eu (III) Chelate Nanoparticles

He Ding¹, Lin Yang¹, Hongshang Peng^{1,*}, Xiaohui Wang¹, Fangtian You¹, and Lingling Hou²

¹Key Laboratory of Luminescence and Optical Information, Ministry of Education, Institute of Optoelectronic Technology, Beijing Jiaotong University, Beijing 100044, China

²College of Life Sciences and Bioengineering, Beijing Jiaotong University, Beijing 100044, China

Eu-tris(dinaphthoylmethane)-bis-(trioctylphosphine oxide) (Eu-DT) molecules encapsulated by Polystyrene and bis(trimethoxysilyl)decane nanoparticles were prepared via a modified encapsulation-precipitation method and show a high sensitivity to sense temperature. After surface modification with poly-*L*-lysine, the fluorescent nanoparticles obtained a well biocompatibility and low toxicity at a certain concentration. In the physiological temperature range (25–45 °C), the fluorescence of the nanoparticles is rather sensitive to temperature with a sensitivity of $-2.6\%/^{\circ}\text{C}$. The temperature nanosensors and gold nanorods were internalized into living HepG2 cells. The fluorescence intensity of phagocytic nanoparticles decreased with the irradiation of 808-nm laser, which were captured by Epi-fluorescence microscope.

Keywords: Gold Nanorods, Photothermal Therapy, Europium Chelate, Temperature Nanosensors, Luminescence.

1. INTRODUCTION

Cancer is one of the most deadly diseases. Many methods of treatment have been established, such as surgical resection, chemotherapy, and radiotherapy; however, traditional methods suffer from side effects. For example, surgical treatment usually results in major trauma, and healthy tissue will be inevitably injured by the high radiation dose in radiotherapy. Laser hyperthermia is a rather mild and non-invasive alternative or complementary treatment that takes advantage of the photothermal effect of light-absorbers localized in malignant tissue to kill tumor cells.^{1–3} In particular, metal nanoparticle (NP)-mediated near-infrared thermal therapies are attractive in that (i) near-infrared light has a large penetration depth in biological tissue and (ii) the surface plasmon resonance (SPR) of metal NPs can efficiently convert the laser radiation into heat.^{4,5} Considerable work has been devoted to this field, but discrepancies in therapeutic parameters (dosage of metal NPs, power and time of irradiation, etc.) among different research groups hinder the advancement of photothermal therapy toward clinical application.^{6–8} Tumor cells are efficiently

destroyed when temperature exceeds 42.5 °C,⁹ and intracellular temperature can thus be used as the basis to evaluate the efficacy of photothermal therapy.^{10,11} Therefore, it would be helpful to standardize these therapeutic parameters if the intracellular temperature can be detected during the course of hyperthermal treatment.

Many fluorescent nanothermometers have been developed to sense temperature including quantum dots,^{7,12} polymer dots,¹³ nanogels,^{2,3} Ln³⁺-based NPs,^{8,14–16} metal-organic frameworks,¹⁷ and fluorescent proteins.¹ However, few of them are capable of intracellular temperature imaging.^{1–3} The challenge may lie in the strict requirements for biocompatibility and spatial and temperature resolution. In previous studies, we have reported a type of luminescent NPs prepared from a visible-light sensitized Eu³⁺ chelate, Eu-tris(dinaphthoylmethane)-bis-(trioctylphosphine oxide) (Eu-DT), for temperature sensing over the physiological range (25–45 °C).^{4,18} Unfortunately, the Eu-DT NPs cannot be internalized by living cells because of the silica nature of the particle surface, and intracellular temperature imaging is unfeasible.

In this work, the luminescent nanothermometer Eu-DT NPs were modified with positively charged poly-*L*-lysine

*Author to whom correspondence should be addressed.

(PLL) molecules by a one-step reprecipitation-encapsulation method.^{5,6} The resultant PLL shell provides the Eu-DT NPs good biocompatibility and high efficiency of cellular uptake without impairing their temperature sensitivity. In addition, gold nanorods (GNRs) with longitudinal surface plasmon resonance (LSPR) absorption at 808 nm were synthesized and modified by methoxy(polyethyleneglycol)-thiol (mPEG₅₀₀₀-SH) to reduce the toxicity and enhance the biocompatibility of GNRs. The cytotoxicities of these two nanoparticles were recorded by the MTT method which is a colorimetric assay for assessing cell viability.

Cancerous cells were co-incubated with PLL-EuDT NPs and GNRs, and irradiated with NIR irradiation for different times. The intracellular temperature was tentatively imaged with an Epi-fluorescence microscope according to the luminescence of Eu-DT NPs. In accordance with the results, Eu-DT NPs exhibit a high sensitivity to temperature alternation within the physiological range.

2. EXPERIMENTAL DETAILS

2.1. Reagents

Polystyrene (PS, $M_w = 280$ kDa), PLL ($M_w = 4\text{--}15$ kDa), gold (III) chloride trihydrate ($\text{HAuCl}_4 \cdot 4\text{H}_2\text{O}$), sodium borohydride (NaBH_4), hexadecyltrimethylammonium bromide (CTAB), silver nitrate (AgNO_3), L-ascorbic acid (LAA), hydrochloric acid (HCl), and tetrahydrofuran (THF) were purchased from Sigma-Aldrich. Methoxy(polyethyleneglycol)-thiol (mPEG₅₀₀₀-SH) and 2-bis(trimethoxysilyl)decane (BTD) were obtained from JenKem Technology Co., Ltd. (China) and Gelest respectively. All chemicals were used without further purification. Eu-DT was prepared as described previously.⁶ Deionized water from the Aquapro ED12-3002-U system was used throughout.

2.2. Synthesis of Gold Nanorods

Gold nanorods were prepared via a two-step seed-mediated growth method.^{19,20} Gold seeds were first synthesized as follows. 0.5 mL of HAuCl_4 (10 mM) and 10 mL of CTAB (0.1 M) were thoroughly mixed at 30 °C. To the resultant mixture, 0.6 mL of ice-cold NaBH_4 (10 mM) was injected quickly under vigorous stirring. The solution was left standing for 2 h at 30 °C, and the pale brown gold seed solution was ready.

In order to prepare gold nanorods, the growth solution was prepared in advance by adding 0.08 mL of AgNO_3 (10 mM) to a well-mixed solution composed of 0.5 mL of HAuCl_4 (10 mM) and 10 mL of CTAB (0.1 M). Then the mixture was acidified by adding 0.2 mL of HCl (1 M) and ultimately clarified with 0.08 mL of ascorbic acid solution (0.1 M). Subsequently, 24 μL of gold seeds were added to the as-prepared growth solution, and gold nanorods were formed after being stirred for 2 h at 30 °C. The gold nanorods were washed twice by centrifugation

(13,000 rpm, 10 min) to remove excess CTAB and re-dispersed in deionized water to be stored at 4 °C for further experiments.

2.3. Surface Modification of Gold Nanorods with Polyethylene Glycol

The gold nanorods obtained as prepared cannot be applied in live cell experiments due to the toxicity of CTAB surfactant introduced by the synthesis of GNRs. To remove the surfactant and improve the biocompatibility of GNRs, 1 mL of mPEG₅₀₀₀-SH (1.2 mM) was added to 10 mL of gold nanorod dispersion. After 24 h stirring at room temperature, the PEG-coated GNRs were collected by centrifuging twice at 13,000 rpm for 10 min to remove the remaining CTAB and excess PEG-peptide and re-dispersed in deionized water to be stored at 4 °C for further experiments.

2.4. Synthesis of Core-Shell Eu-DT NPs

In a typical experiment, Eu-DT, PS, and BTD were dissolved in THF, in a 15:35:50 weight ratio with a total concentration of 200 ppm. Then, 1 mL of the stock solution was rapidly injected into 8 mL of water containing 0.16 mg PLL (pH 9, adjusted by ammonium hydroxide) under sonication. The resulting suspensions were left to stand for 2 h at 4 °C. Subsequently, the organic solvent was removed by dialyzing against water for 24 h. The final resulting suspension (containing around 35 mg of NPs per liter) was stored at 4 °C for the further experiments, including SEM, TEM, zeta potential, temperature calibration, cell incubation, and microscopy observation.

2.5. Characterization

SEM images were obtained with a field emission scanning electron microscope (FE-SEM) (JEOL JSM-7500F), using an aqueous dispersion of NPs placed on the microscope specimen support (aluminum). The dispersion was subsequently evaporated at room temperature and coated with Au. For TEM characterization, the specimen was prepared by placing an aqueous dispersion of NPs on a fresh copper mesh, and then drying at room temperature. TEM images were recorded using an electron microscope (Tecnai 20, FEI) at an acceleration voltage of 120 kV. Zeta potentials and hydrodynamic size were determined by photon correlation spectroscopy and by dynamic light scattering (DLS) respectively, using a Zetasizer Nano instrument (Malvern Instruments, Malvern, UK). Ultraviolet-visible (UV-vis) absorption spectra and fluorescence spectra were recorded on a UV-3101PC spectrophotometer (Shimadzu) and an F-4500 fluorescence spectrophotometer (Hitachi), respectively.

2.6. Temperature Calibration of Eu-DT NPs *In Vitro*

For the laser irradiation experiment, a continuous-wave fiber-coupled diode laser with a wavelength of 808 nm

was used. An aqueous solution of polyvinyl alcohol (PVA) was used to simulate the cell environment. 0.5 mL of PVA (10 wt%), 0.4 mL of aqueous Eu-DT nanoparticle solution, and 0.1 mL of gold nanorods (OD = 6) were mixed in the cuvette. Under near infrared (NIR) irradiation ($\sim 0.4 \text{ W/cm}^2$), the spectra of Eu-DT nanoparticles were measured at different irradiation times.

The length of NIR irradiation may raise the temperature of the aqueous solution. Hence a controlled trial was performed without gold nanorods. The procedures are similar to above temperature calibration except that the aqueous solution of gold nanorods is replaced by water with the same volume.

2.7. Cells Culture and Cytotoxicity of NPs

HepG2 cells were grown in 6 cm cell glass-bottom culture dishes in RPMI-1640 cell medium supplemented with 10% FBS at 37 °C under humid conditions with CO₂ (5%). The cytotoxicity of the PLL-coated Eu-DT NPs and the PEG-modified GNRs was evaluated using the MTT assay. HepG2 cells were seeded on a 96-well microtiter plate at approximately 5000 cells per well, and incubated 12 h to allow the cells to attach to the well. The 96 wells were classified into six groups, with one group left blank for control. The PLL-coated Eu-DT NPs/PEG-modified GNR aqueous dispersions were sterilized by UV illumination for 10 min before loading. Then, NP suspensions with different volumes of NPs were added in sequence into respective wells, while the total volume was kept constant at 200 μL by decreasing the quantity of culture medium. After incubation for 12 h, 10 μL of 3-(4,5-dimethylthiazol-2-yl)-2,5-diphenyltetrazolium bromide (MTT, 5 mg/mL in phosphate buffered saline solution, pH 7.4) was added to each well. The microtiter plate was further incubated for 4 h to allow the MTT to be metabolized. Then the mixed solution was dumped off and formazan (MTT metabolic product) was dissolved by adding 100 μL /well dimethyl sulfoxide (DMSO). After being shaken for 5 min, optical density (OD) was measured spectrophotometrically in an ELISA reader (BioTek, ELx800™) at a wavelengths of 490 nm (test) and 630 nm (reference). The relative cell viability (%) related to the control wells containing cell culture medium without NPs was calculated by $\text{OD (test)}/\text{OD (control)} \times 100$.

2.8. Temperature Sensitivity Experiment in Cell

HepG2 cells were cultured in 6 cm cell bottom culture dishes for 24 h (37 °C, 5% CO₂), then PEG-modified gold nanorods and Eu-DT nanoparticles were loaded. After 24 h, the culture plates were washed twice with PBS solution before the NIR irradiation. Then, HepG2 cells were exposed under the NIR irradiation (a continuous-wave fiber-coupled diode laser with wave-length 808 nm, $\sim 0.4 \text{ w/cm}^2$), and the cellular imaging was performed on a Nikon ECLIPSE TE2000-S. The fluorescence pictures are

taken every 2 minutes during NIR irradiation, with 380-nm excitation.

3. RESULTS AND DISCUSSION

3.1. Preparation of PEG-Modified Gold Nanorods

Figure 1 shows a transmission electron microscopy (TEM) image and extinction spectrum of the as-prepared gold nanorods. The aspect ratio (R) of the gold nanorods is estimated to be 4.1 ± 0.3 from the TEM image. The maximum absorption (λ_{max}) at longitudinal SPR is thus calculated to be $\sim 809 \text{ nm}$ according to the expression of $\lambda_{\text{max}} = 95R + 420$.²¹ This result is in good agreement with that experimentally obtained from Figure 1(B).

It is known that the as-prepared gold nanorods stabilized by CTAB are cytotoxic in biological applications. Hence, CTAB is generally replaced by biocompatible molecules, such as thiol-PEG that exhibits affinity for the gold nanorod surface.²² This can be easily achieved by mixing mPEG-SH with the GNR dispersion and subsequent centrifugation. Figure 2 shows the zeta potentials of gold nanorods before and after mPEG-SH modification. The transition of zeta potential from 45.5 mV to 1.95 mV indicates that the initial cationic surface is nearly neutral, corresponding to the substitution of CTAB with mPEG-SH.

3.2. Synthesis of Core-Shell Sensing NPs

The core-shell Eu-DT NPs were synthesized according to previously reported PLL-assisted encapsulation-precipitation method.²³ Because of the introduction

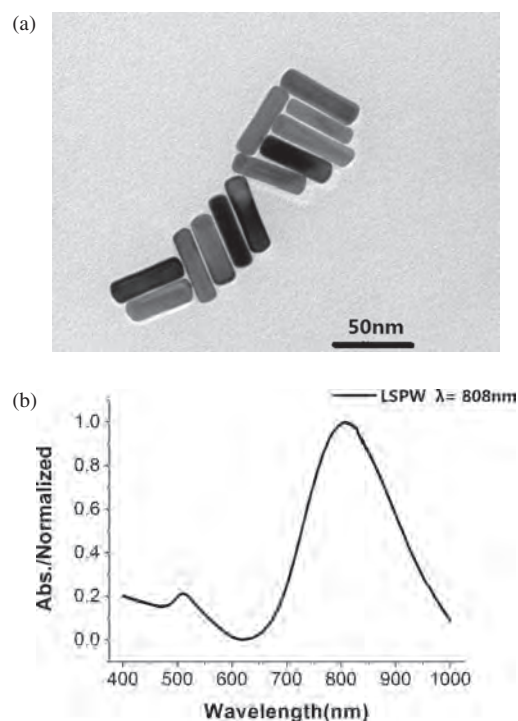


Figure 1. TEM image (A) and normalized extinction spectrum (B) of gold nanorods.

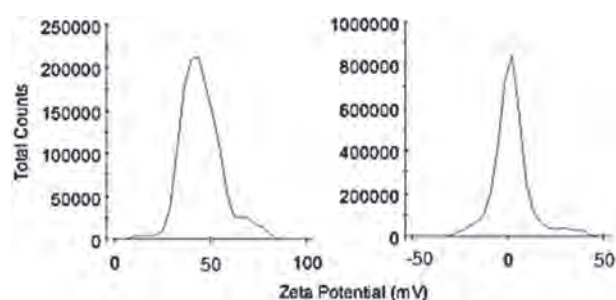


Figure 2. The zeta potential of gold nanorods dispersions before and after PEG modification (measured at 25 °C). The zeta potential values are determined to be 45.5 mV (left) and 1.95 mV (right) respectively.

of cationic polymer molecules, the initially negatively charged Eu-DT NPs were coated *in situ* with a PLL layer via electronic force between amino groups and silanol groups. Figure 3(A) clearly shows the presence of an outer layer around the particle core, indicating successful PLL coating. Moreover, the existence of the PLL shell is also verified by the sharp transition of zeta potentials from -37.4 to 45.5 mV Figure 3(B). The positive net charge is favorable for the NPs to interact with the negative cell membrane, resulting in cellular uptake.

3.3. Cytotoxicity of PEG-Modified Gold Nanorods/PLL-Coated Eu-DT NPs

The potential cytotoxic effects of the PEG-modified GNRs and PLL-coated Eu-DT NPs were tested by using an

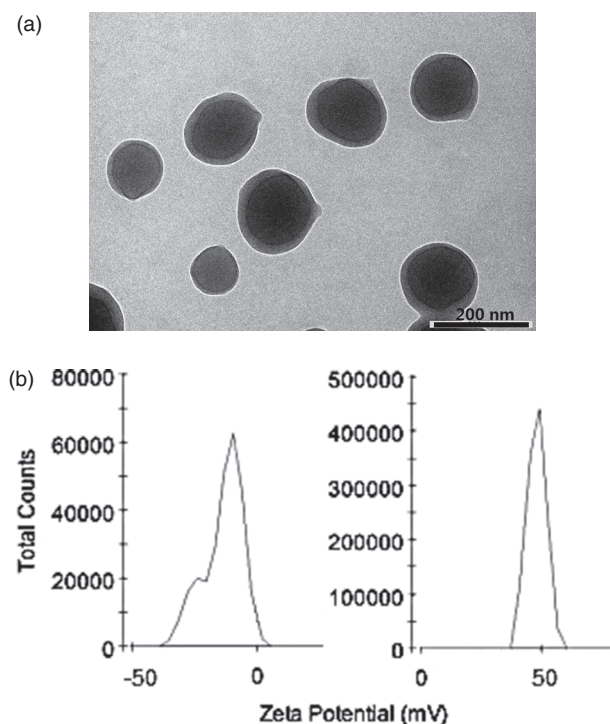


Figure 3. (A) TEM image of PLL-coated Eu-DT NPs; (B) zeta potentials of Eu-DT NPs before (left) and after (right) PLL coating.

MTT assay. Living human hepatocellular liver carcinoma (HepG2) cells were incubated with the NP aqueous dispersion for 12 h, and then their mitochondria and metabolic activities were examined after exposure to the complex of 3-(4,5-dimethylthiazol-2-yl)-2,5-diphenyltetrazolium bromide (MTT). As shown in Figure 4, loading of gold nanorods with an optical density between 0.18 and 0.36 give rise to relative lower inhibition to cells, and for PLL-NPs the concentration range is from 6 to 14 $\mu\text{g/mL}$. In the following intracellular experiments, gold nanorods with OD = 0.6 and a dosage of 10 $\mu\text{g/mL}$ of Eu-DT NPs were used.

3.4. Temperature Sensitivity of PLL-Coated Eu-DT NPs

Temperature sensitivity of Eu-DT NPs was studied by measuring the response of emission spectra and intensity. The emission spectra of Eu-DT NPs displayed in Figure 5(A) were recorded under 318 nm excitation. The intensity—as calculated by integrating fluorescence spectra—decreases rapidly by more than 62% as temperature increases from 24 to 51 °C. Figure 5(B) shows the emission intensity of Eu-DT NPs recorded in the temperature range of 25–50 °C. In this temperature range, the fluorescent intensity decreases by 65% with the temperature (a linear relationship), yielding a temperature sensitivity of $-2.6\%/^{\circ}\text{C}$.

3.5. Plasmonic Photothermal Experiment

The gold nanorod could generate huge heat under NIR laser irradiation. By using of Eu-DT NPs which are

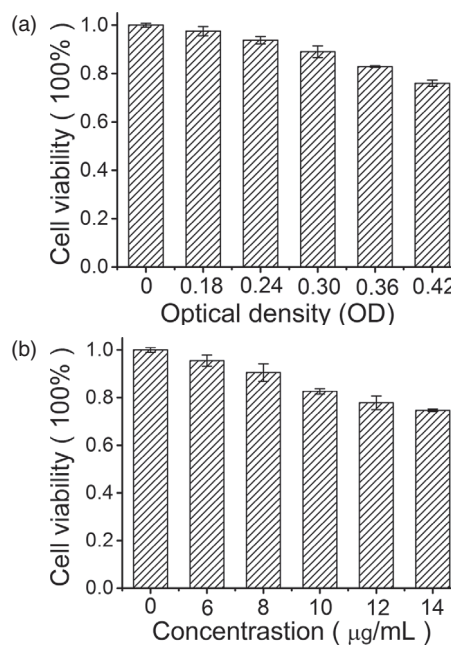


Figure 4. HepG2 cell viability determined by MTT assay with (A) PEG-modified gold nanorods and (B) PLL-coated Eu-DT NPs. Cells loaded with NPs at different concentrations are incubated with MTT for 4–6 h.

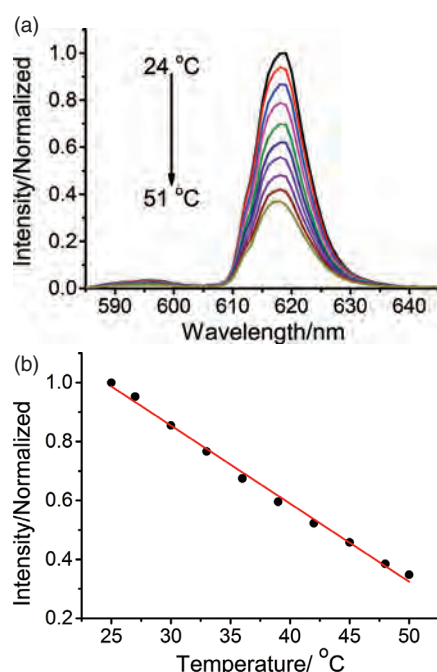


Figure 5. Temperature sensing Eu-DT NP aqueous dispersion: (A) emission spectra and (B) emission intensity under 381 nm excitation at different temperatures.

sensitive to temperature, the temperature induced by gold nanorods under different NIR irradiation times could be detected. Figure 6(A) shows the luminescent intensity of the GNR and Eu-DT NP mixture with different NIR

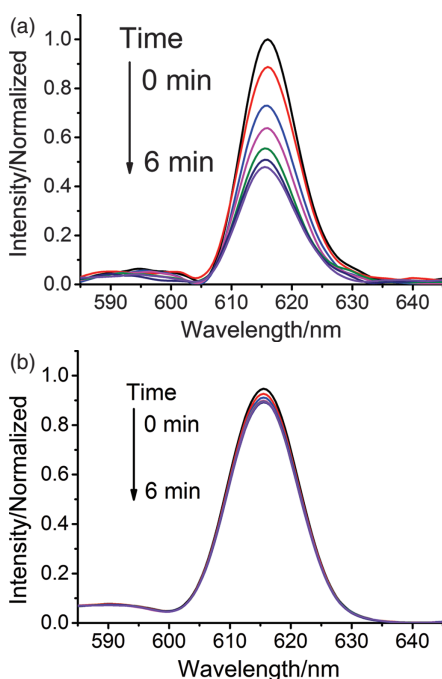


Figure 6. Emission spectra under 381 nm excitation under different NIR irradiation: (A) temperature sensing Eu-DT NPs and gold nanorods aqueous dispersion and (B) only temperature sensing Eu-DT NPs aqueous dispersion.

Table I. Temperature per minute under NIR irradiation at (A) the whole area and (B) the local area.

A (°C)	26	30	33	34.7	36.1	37.2	37.9	38.5
B (°C)	25	40	52	57	60	63	66	68

irradiation times. As NIR irradiation time increased, the luminescent intensity of Eu-DT NPs decreased, indicating the temperature was increased due to photothermal effect. It needs to point out that NIR irradiation solely may elevate the temperature of solution. So a controlled trial without GNR is needed to adjust this error. Figure 6(B) shows that the temperature of aqueous solution did not change much. Finally, the temperature of the gold nanorods under different irradiation times can be calculated by the related luminescent intensity of Eu-DT.

Meanwhile, we measured the whole area temperature of the solution with a thermoelectric thermometer. This method can also detect the local area temperature with the luminous change of Eu-DT NPs. The very interesting phenomenon is that the temperature of the whole area was different from the temperature of the local area under the same conditions. Table I shows the temperature in the two different measured methods under the NIR irradiation. As the NIR irradiation time increased, the temperatures in both of the two methods increased. However, the whole area temperature changed slowly. On the contrary, the local temperature changed rapidly (Table I). This means the heat could not spread to the whole area in a very short time. With this characteristic, it is expected that the tumors

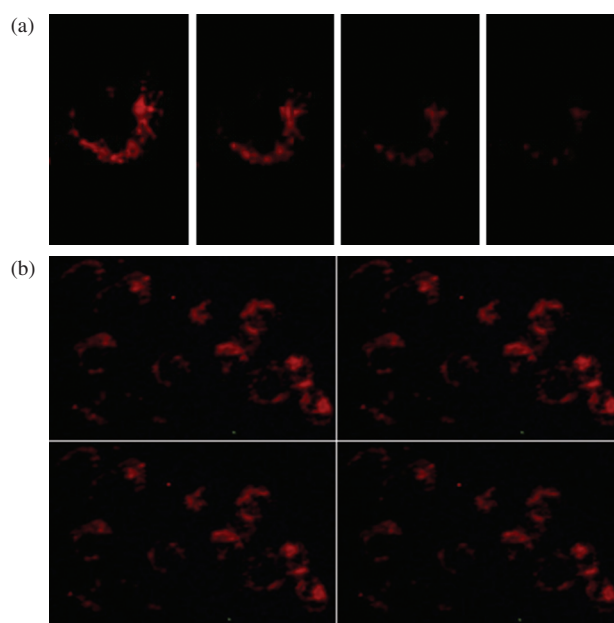


Figure 7. Fluorescence images of HepG2 cells loaded with 11.6 $\mu\text{g/mL}$ of sensing PLL coating Eu-DT NPs (A) with and (B) without gold nanorods.

cells can be killed without hurting surrounding healthy cells.

According to the previous experiments, photothermal effect based on gold nanorods was performed in cells condition. Figure 7 shows the fluorescence images of Eu-DT NPs incubated in the HepG2 cells with and without the gold nanorods under the NIR irradiation. From the four images in Figure 7(A), the intensity of luminescence decreased with increasing irradiation time because the gold nanorods generated heat under the NIR irradiation. Conversely, without gold nanorods, the luminescent intensity of Eu-DT NPs in HepG2 cells had almost no change. The results of luminescent Eu-DT NPs in the HepG2 cells are similar to aforementioned *in vitro* experiments. In conclusion, a precise fluorescent method to detect intracellular temperature during PDT was established by using of luminescent Eu-DT NPs. More details will be introduced in the future.

4. CONCLUSIONS

In conclusion, a luminescent nanoparticle was easily prepared for detecting the photothermal effect of gold nanorods. The sensing NPs are composed of Eu-DT whose luminescence is very sensitive to temperature, with a temperature sensitivity of $-2.6\%/^{\circ}\text{C}$. Gold nanorods with longitudinal surface plasmon wavelength (LSPW) at 808 nm was synthesized and exploited as PDT agents. Under 808-nm NIR irradiation, both the *in vitro* temperature and *in vivo* temperature induced by GNRs were sensed by DT-Eu NPs. This work is helpful to optimize the efficacy of PDT therapy by accurately monitoring intracellular temperature.

Acknowledgments: This work was financially supported by NSFC (61078069), NCET (12-0771), National Science Fund for Distinguished Young Scholars (61125505), and Fundamental Research Funds for the Central Universities (2010JBZ006).

References and Notes

1. J. S. Donner, S. A. Thompson, M. P. Kreuzer, G. Baffou, and R. Quidant, *Nano Lett.* 12, 2107 (2012).
2. C. Gota, K. Okabe, T. Funatsu, Y. Harada, and S. Uchiyama, *J. Am. Chem. Soc.* 131, 2766 (2009).
3. K. Okabe, N. Inada, C. Gota, Y. Harada, T. Funatsu, and S. Uchiyama, *Nat. Commun.* 3, 705 (2012).
4. O. Ekici, R. K. Harrison, N. J. Durr, D. S. Eversole, M. Lee, and A. Ben-Yakar, *J. Phys. D: Appl. Phys.* 41, 185501 (2008).
5. W. Jo, K. Freedman, D. K. Yi, R. K. Bose, K. K. Lau, S. D. Solomon, and M. J. Kim, *Biofabrication* 3, 015002 (2011).
6. H. Peng, M. I. Stich, J. Yu, L. N. Sun, L. H. Fischer, and O. S. Wolfbeis, *Adv. Mater.* 22, 716 (2010).
7. L. M. Maestro, E. M. Rodriguez, F. S. Rodriguez, M. C. la Cruz, A. Juarranz, R. Naccache, F. Vetrone, D. Jaque, J. A. Capobianco, and J. G. Sole, *Nano Lett.* 10, 5109 (2010).
8. D. Jaque and F. Vetrone, *Nanoscale* 4, 4301 (2012).
9. T. C. Shih, P. Yuan, W. L. Lin, and H. S. Kou, *Med. Eng. Phys.* 29, 946 (2007).
10. K. Xia, L. Zhang, Y. Huang, and Z. Lu, *J. Nanosci. Nanotechnol.* 15, 63 (2015).
11. S. Mallick, I. C. Sun, K. Kim, and D. K. Yil, *J. Nanosci. Nanotechnol.* 13, 3223 (2013).
12. J. M. Yang, H. Yang, and L. Lin, *ACS Nano* 5, 5067 (2011).
13. F. Ye, C. Wu, Y. Jin, Y. H. Chan, X. Zhang, and D. T. Chiu, *J. Am. Chem. Soc.* 133, 8146 (2011).
14. C. D. Brites, P. P. Lima, N. J. Silva, A. Millán, V. S. Amaral, F. Palacio, and L. D. Carlos, *Adv. Mater.* 22, 4499 (2010).
15. F. Vetrone, R. Naccache, A. Zamarron, A. Juarranz de la Fuente, F. Sanz-Rodríguez, L. M. Maestro, E. M. Rodriguez, D. Jaque, J. G. Sole, and J. A. Capobianco, *ACS nano* 4, 3254 (2010).
16. L. H. Fischer, G. S. Harms, and O. S. Wolfbeis, *Angew. Chem. Int. Ed.* 50, 4546 (2011).
17. Y. Cui, H. Xu, Y. Yue, Z. Guo, J. Yu, Z. Chen, J. Gao, Y. Yang, G. Qian, and B. Chen, *J. Am. Chem. Soc.* 134, 3979 (2012).
18. H.-S. Peng, S.-H. Huang, and O. S. Wolfbeis, *J. Nanopart. Res.* 12, 2729 (2010).
19. B. Nikoobakht and M. A. El-Sayed, *Chem. Mater.* 15, 1957 (2003).
20. B. Altansukh, J. Yao, and D. Wang, *J. Nanosci. Nanotechnol.* 9, 1300 (2009).
21. X. Huang, S. Neretina, and M. A. El-Sayed, *Adv. Mater.* 21, 4880 (2009).
22. T. Niidome, M. Yamagata, Y. Okamoto, Y. Akiyama, H. Takahashi, T. Kawano, Y. Katayama, and Y. Niidome, *J. Controlled Release* 114, 343 (2006).
23. X.-H. Wang, H.-S. Peng, L. Yang, F.-T. You, F. Teng, A.-W. Tang, F.-J. Zhang, and X.-H. Li, *J. Mater. Chem. B* 1, 5143 (2013).

Received: xx Xxxx 2014. Accepted: 12 Xxxx 2014.